Reduce Distillation Column Cost by Hybrid Particle Swarm and Ant Colony Optimization Technique

Sandip Kumar Lahiri[2] and Chinmaya Prasad Lenka[1,*]

[1]*Improvement Engineer, Sadara Chemical Company, Saudi Arabia*

[2]*Manager, Scientific Design, USA*

Abstract: A novel method for optimum design of plate type distillation column integrating the equilibrium, hydraulic and economic calculations is presented in the present paper. The present study explores the use of non-traditional optimization technique: called hybrid Particle swarm optimization (PSO) and Ant colony optimization (ACO), for design optimization of plate type distillation column from economic point of view. The optimization procedure involves the selection of the major plate geometric parameters such as hole diameters, ratio of downcomer area to tower area, weir height, fractional hole area in tray, tray spacing, tower diameter etc. and minimization of total annual cost is considered as design target subjected to operational constraints like flooding, weeping entrainment, quality specifications etc. The solution space of such type of problem is very complex due to presence of various nonlinear constraints and multiple minima. Hybrid Particle swarm optimization and Ant colony optimization (PSACO) technique is applied to deal with such complexity. The particle swarm optimization applies for global optimization and ant colony approach is employed to update positions of particles to attain rapidly the feasible solution space. Ant colony optimization works as a local search, wherein, ants apply pheromone-guided mechanism to update the positions found by the particles in the earlier stage. The presented hybrid Particle swarm optimization and Ant colony optimization (PSACO) technique is simple in concept, few in parameters and easy for implementations. Furthermore, the PSACO algorithm explores the good quality solutions quickly, giving the designer more degrees of freedom in the final choice with respect to traditional methods. One case study is presented to demonstrate the effectiveness and accuracy of proposed algorithm. The PSACO approach is able to reduce the total cost of distillation column as compare to cost obtained by commercial simulator.

Keywords: Particle swarm optimization, ant colony optimization, hybrid particle swarm and ant colony optimization, distillation column design, plate type distillation column.

1. INTRODUCTION

Cut throat global competition and shrinking profit margin forced the chemical process industries (CPI) to introspect the traditional design methodology of process equipments and compel the designer to take cost (both initial capital cost and future energy cost) as important design criteria during design phase. Plate type distillation columns (PTDC) are not only contributed a major portion of capital investment in new projects but also the major consumers of energy in CPI. Because of their sheer large numbers in any CPI, small improvement in plate type distillation column design strategies offer big saving opportunities. Computer software marketed by companies such as Aspen plus, Hysys and PRO-II are used extensively in the design and rating of plate type distillation column. The classical approach to plate type distillation column (PTDC) design in these simulators involves a significant amount of trial-and-error because an acceptable design needs to satisfy a number of constraints (e.g. product purity specifications, flooding, entrainment, downcomer velocity, utilities constraints, weeping and allowable pressure drops etc.) (Kister 1992) [1]. Various design options for the distillation column including the variations in the hole diameter, tray spacing, ratio of downcomer area to column area, fractional hole area based on active area etc. are incorporated in these software as an user input. Typically, for hydraulic calculations, a designer chooses various geometrical parameters mentioned above based on experience or heuristic to arrive at a possible design. The final design should satisfy a number of hydraulic constraints such as percentage jet flooding, maximum downcomer velocity, minimum downcomer back up, maximum liquid flow rate per unit length of weir, actual minimum vapor velocity to avoid weeping etc. (Kister 1992) [1]. This will ensure that the distillation unit will perform well in actual plant. If the design does not satisfy the constraints, a new set of geometrical parameters must be chosen to check if there is any possibility of reducing the distillation column cost while satisfying the constraints. Although well proven, this kind of approach is time consuming and may not lead to cost effective design as no cost criteria are explicitly accounted for. Since several discrete combinations of the design configurations are possible, the designer needs an efficient strategy to quickly locate the design configuration having the minimum column cost. Thus the optimal design of plate type distillation column (PTDC) can be posed as a large scale, discrete, combinatorial optimization problem.

*Address correspondence to this author at the Improvement Engineer, Sadara Chemical Company, Saudi Arabia; Tel: 00966-531906875;
Fax: 00966133512533; E-mail: chinu4007@gmail.com

E-ISSN: 2409-983X/16

In literature, attempts to automate and optimize the PTDC design process have been proposed for a long time and subject is still evolving. Sinnot (1989) [2] suggested the hydraulic calculations of distillation column and continuously modify the sizing parameters like column diameter, downcomer area, tray spacing etc. to meet various constraints to avoid flooding, entrainment, weeping etc. Kister (1992) [1] has provided a detailed hydraulic design methods based on empirical equations provided by various researchers over the decades. Detailed design companies across the world use their own correlations and own heuristic to arrive at a functionally acceptable design. Again, designers have to continuously evolve the design parameters to meet various constraints. To improve and optimize such design, Luyben (2006) [3] has incorporated a cost function to evaluate the final design. Main aim is to evaluate the total number of trays, reflux ratio, tray diameter and feed tray location of the column using Aspen plus simulator, which corresponds to a minimum total annual cost. Detail of hydraulic calculations and evaluation of tray and hydraulic parameters are not included in his design. As seen from literatures, the detail tray hydraulic calculations with cost as design criteria is an unexplored area of research.

The limited available published literatures to evaluate optimum reflux ratio and number of trays normally used traditional optimization technique (Luyben 2006) [3]. Most of the traditional optimization techniques based on gradient methods have the possibility of getting trapped at local optimum depending upon the degree of non-linearity and initial guess. Typical properties of such problems are the existence of discontinuities, the lack of analytical representation of the objective function, complex cost function, multiple minima and noise dissemination. Hence, these traditional optimization techniques do not ensure global optimum and also have limited applications.

In these circumstances, the applicability and efficiency of classical optimization algorithms are questionable, giving rise to the need for the development of different optimization methods. Particle swarm optimization (PSO) was developed (Kennedy and Eberhart 1995) [4] as a stochastic optimization algorithm based on social simulation models. Since its development, PSO has gained wide recognition due to its ability to provide solutions efficiently, requiring only minimal implementation effort. This is reflected by increasing number of journal papers with the term "particle swarm" in their titles published by three major publishers, namely Elsevier, Springer, and IEEE, during the years 2000-2014. Also, the potential of PSO for straightforward parallelization, as well as its plasticity, i.e., the ability to adapt easily its components and operators to assume a desired form implied by the problem at hand, has placed PSO in a salient position among intelligent optimization algorithms.

In the early 1990s, ant colony optimization (ACO) was introduced by M. Dorigo, (1992) [5] as a novel nature- inspired metaheuristic for the solution of hard combinatorial optimization (CO) problems. ACO belongs to the class of metaheuristics, which are approximate algorithms used to obtain good enough solutions to hard CO problems in a reasonable amount of computation time. The inspiring source of ACO is the foraging behavior of real ants. When searching for food, ants initially explore the area surrounding their nest in a random manner. As soon as an ant finds a food source, it evaluates the quantity and the quality of the food and carries some of it back to the nest. During the return trip, the ant deposits a chemical pheromone trail on the ground. The quantity of pheromone deposited, which may depend on the quantity and quality of the food, will guide other ants to the food source. As it has been shown in (Dorigo *et al*. 1999)[6], indirect communication between the ants *via* pheromone trails enables them to find shortest paths between their nest and food sources. This characteristic of real ant colonies is exploited in artificial ant colonies in order to solve CO problems (Shelokar *et al*. 2007) [7].

It is known that the PSO may perform better than the EAs in the early iterations, but it does not appear competitive when the number of iterations increases (Angeline 1998) [8]. To improve this character of PSO, one of the methods is hybridizing PSO with other approaches such as ACO (Kaveh and Talatahari 2008)[9]. The resulted method, called Particle Swarm Ant Colony Optimization (PSACO), was initially introduced by Shelokar *et al*. (2007) [7] for solving the continuous unconstrained problems and by Mozafari *et al*. (2006) [10] for reactive power market simulation. PSACO utilized PSO as a global search and the idea of ant colony approach worked as a local search and updated the positions of the particles by applied pheromone-guided mechanism.

In view of the encouraging results found out by the above researchers, an attempt has been made in the present study to apply a new strategy called Particle

Swarm Ant Colony Optimization (PSACO) to the plate type distillation column (PTDC) design problem. The main objective of this study is to explore the effectiveness of this new technique in the design optimization of PTDC from economic point of view. Ability of the hybrid PSACO based technique is demonstrated using case study.

The paper is organized as follows: section 2 describes design of optimum PTDC; Section 3 illustrates the case study and various constraints used in this study to optimally design the PTDC. The brief introduction of PSO, ACO and hybrid PSACO is given in section 4. Section 5 illustrates the application of the PSACO algorithm in case study. Sections 6 summarize the results and advantages of such applications in PTDC design. Finally Section 7 gives a summary of the study.

2. THE OPTIMAL DISTILLATION COLUMN DESIGN PROBLEM

Traditional design approaches (Kister1992, Sinnot1989) [1, 2] are based on iterative procedures which gradually change the design and geometric parameters of tray until satisfy a given quality specification and set of hydraulic and operational constraints like flooding, weeping, entrainment etc. As explained earlier, the traditional hydraulic method of PTDC design (Kister1992) [1] does not take into account the cost function during design stage. The proposed new optimization procedure involves the selection of the major plate geometric parameters such as hole diameters, ratio of downcomer area to tower area, weir height, fractional hole area in tray, tray spacing, tower diameter etc. and minimization of total annual cost is considered as design target subjected to operational constraints like flooding, weeping entrainment, quality specifications etc.

The procedure for optimal PTDC design includes the following step:

a. Simulation of column in any commercial simulators (Aspen plus, Hysys or PRO-II) for the product purity required.

b. Estimation of maximum and minimum vapor and liquid flow rates for the turndown ratio required.

c. Collection of physical properties from the above converged column simulation.

d. Make a trial plate layout: column diameter, down comer area, active area, hole area, hole size, weir height etc. and select a trial plate spacing (values of all the search variables given in Table **1** is assumed within their specified limit).

Table 1: Optimization Variables with their Upper and Lower Limit

Optimization Variable	Variable Notation	Variable Name	Lower and Upper Limit
x_1	d_t	Tower diameter (m)	d_{min} -12.2
x_2	tray space	Tray spacing (m)	0.406-0.914
x_3	v type	valve type (0=sieve, 1=round, 2=rectangular)	0-0
x_4	φ	Hole area (fraction of bubbling area)	0.08-0.15
x_5	d_h	Hole diameter (m)	0.00317-0.0254
x_6	$deck_t$	Deck thickness (m)	0.00094-0.00635
x_7	passcfg	Pass configuration	0.0254-0.0762
x_8	h_w	Outlet weir height (m)	0.0381-0.0889
x_9	w_{dct}	Top downcomer (DC) width (m)	$0.11(d_t)$-$0.20(d_t)$
x_{10}	w_{dcb}	Bottom DC width (m)	$0.11(12d_t)$-$0.20(12d_t)$
x_{11}	w_{dcs}	Bottom DC sump width (m, 0=none)	0-0
x_{12}	c_{dc}	DC clearance (m)	0.0254-0.0762
x_{13}	ch_w	Center outlet weir height (m)	0.0381-0.0889
x_{14}	w_{cdct}	Top center DC width (m)	$0.11(d_t)$-$0.20(d_t)$
x_{15}	w_{cdcb}	Bottom center DC width (m)	$0.25(d_t)$-$0.49(d_t)$
x_{16}	w_{cdcs}	Bottom center DC sump width (m, 0=none)	0-0
x_{17}	c_w	Center DC clearance (m)	0.0254-0.0762
x_{18}	stgno	Total number of stage (-)	10-35
x_{19}	feedstg	Feed stage number from top (-)	4-23

Table 2: Different Constraints and Their Limit

Optimization Variable	Variable Notation	Variable Name	Lower and Upper Limit
g_1	%Jet flood	Final percent of jet flood by most appropriate method (%)	40-80
g_2	%Downcomer flood	Glitch method percent downcomer flood (%)	0-50
g_3	%Downcomer Back up	Glitsch method DC backup as % of tray spacing (%)	0-50
g_4	Weir load	Weir loading (gpm/in weir)	2-13
g_5	u_{ldc}	Clear liquid downcomer entrance velocity (m/s)	0-0.1524
g_6	d*p*	tray pressure drop (Pa)	0-1034.25
g_7	ar_{dct}	Top Downcomer to tower area ratio (%)	8-20
g_8	ar_{dcb}	Bottom Downcomer to tower area ratio (%)	8-20
g_9	FPL	Flow path length (m)	0.457-2.54
g_{10}	w_{frac}	Weep fraction	0-0.25
g_{11}	e_{frac}	Entrainment fraction (of vapor rate)	0-0.1

e. Estimation of all the constraints given in Table **2** such as jet flood percentage, downcomer flood percentage, down comer back up, weep fraction, entrainment fraction, pressure drop etc. by using various correlations given in appendix 1.

f. Evaluation of the capital investment, operating cost and the objective function.

g. Utilization of the optimization algorithm to select a new set of values for the design variables (given in Table **1**) until all the constraints (given in Table **2**) are within their specified limits.

h. Iterations of the previous steps until a minimum of the objective function is found

i. Finalize design: draw up the plate specification and sketch the layout.

3. CASE STUDY

To demonstrate the effectiveness of proposed algorithm, a multicomponent distillation problem was chosen from Literature (Filipe Soares Pinto, Roger Zemp, Megan Jobson, Robin Smith, 2011)[11]. Present work has taken into account the detail hydraulic calculations and implement hybrid PSACO algorithm to optimize the cost. Same cost function was used in present study as in Luyben (2006)[3]. For simplicity 5 component distillation column has chosen, however, present algorithm can also be easily applied to complex multi component distillation also.

3.1. Distillation Problem Description

A lowest cost plate type distillation column has to be designed to separate a 5 component mixture of 10 mole% propene, 20 mole% propane, 40 mole% isobutane, 20 mole% n-butane and 10 mole% n-pentane. Feed rate is 1000kmol/hr. with 0.4 vapor fraction and feed temperature and pressure are 24.95^{0}C and 400kPA respectively. Final product quality specifications are 99.5% top recovery of n-butane and 99.5% bottom recovery of n-pentane. As a starting, base case distillation column has 29 theoretical stages with feed stage location 11 from top. Number of stages and feed stage location can be varied to design the lowest cost column.

The original problem can be set as;

$$Minimize\ \ Total\ \ cost,\ \ C_{tot}(x)\ where\ x_j^L \le x_j \le x_j^U \quad j=1,2,...,N$$
$$Subject\ to\ g_i(x) \le 0\ where\ i=1,2,...,m$$

Where x is the vector of optimization variables as given in Table **1** with their corresponding lower $\left(x_j^L\right)$ and upper limits $\left(x_j^U\right)$. Total cost C_{tot} is taken as the objective function and detail given in section 3.1. The set of constraints g(x) are given in Table **2** along with their limits. The calculations of the constraints are summarized in appendix 1 and the meaning of the constraints summarized in section 3.3. These constraints are then converted to inequalities in same format as stated above with the help of their limits (Table **2**). Considering minimization of PTDC cost as the objective function, improved version of Particle swarm optimization technique is applied to find the

optimum design configuration with product purity and hydraulic parameters (Table **2**) as the constraint.

3.2. Objective Function

Total cost C_{tot} is taken as the objective function, which includes capital investment (C_{cap}), energy cost (C_e);

$$C_{tot} = \frac{C_{cap}}{Payback\ period} + C_e \quad (1)$$

Capital investment includes column capital cost, (C_{col}) and reboiler and condenser capital cost, (C_{HE});

$$C_{cap} = C_{col} + C_{HE} \quad (2)$$

Column capital cost depends on column height and diameter as follows:

$$C_{col} = 17640 d_t^{1.006} H^{0.802} \quad (3)$$

Where d_t diameter and H tower is column height.

$$H = 1.2\left(N_{stage} - 2\right)S_{tray} \quad (4)$$

Where N_{stage} is total number of stages and S_{tray} is tray spacing.

Heat exchanger capital cost can be calculated as follows:

$$C_{HE} = 7296\left(Area_{condenser} + Area_{Reboiler}\right)^{0.65} \quad (5)$$

Where;

$$Area_{condenser} = \frac{Q_{condenser}}{U\Delta t} = \frac{Q_{condenser}}{(852)(13.9)} \quad (6)$$

$$Area_{reboiler} = \frac{Q_{reboiler}}{U\Delta t} = \frac{Q_{reboiler}}{(568)(34.8)} \quad (7)$$

Energy cost is given by;

$$C_E = Q_{Reboiler} H C_{steam} \quad (8)$$

Where H is operating hours and C_{steam} is unit cost of steam.

3.3. Search Optimization Variables

The various search optimization variables are tabulated in Table **1** along with their lower and upper bounds. These upper and lower bounds are taken as per broad guidelines given by Kister(1992) & Sinnot(1989) [1, 2]. In some instances, best practices of industrial design companies are also followed to set the limits of these variables. For column diameter, a minimum diameter (d_{min}) is calculated based on 80% jet flooding criteria (Kister 1992) [1].

The pass configuration field designates one or two pass trays and the specific orientation for two pass trays. A value of 1 designates a one-pass tray and is the default if an entry error is made. A value of 2A designates a two-pass tray with liquid flowing from the center to the side downcomer. A field value of 2B designates a two-pass tray with liquid flowing from the side to the center downcomer.

3.4. Operational and Hydraulic Constraints

Though lowest cost column which obey the product purity specifications is the main selection criteria for PTDC but this is not the only criteria for commercial plants. The concept of a good design involves aspects that cannot be easily described in a single economic objective function e.g. flooding, entrainment, weeping, pressure drop, tray geometric constraints etc. These criteria though empirical have a profound effect on PTDC performance in commercial plants. Operating limit of distillation tray is shown in the schematic of Figure **1**.These criteria are sometimes expressed as geometric, hydraulic and service constraints. Following section briefly describe the various constraints used in the present study. More detail can be found in (Kister 1992, Sinnot 1989) [1, 2].

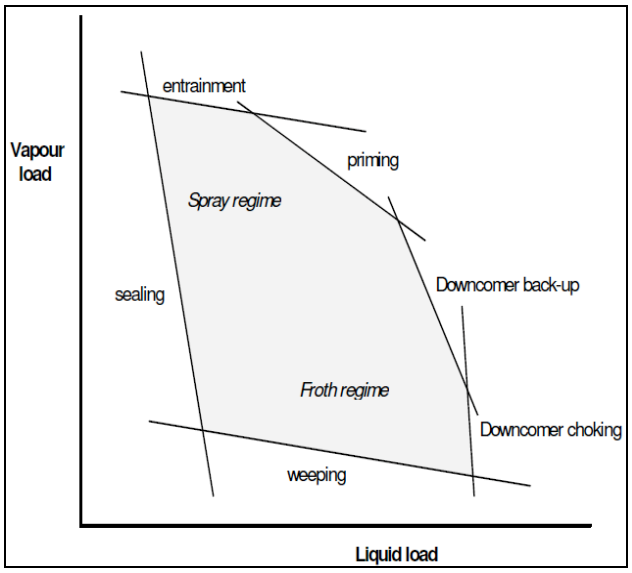

Figure 1: Operating limit of a distillation column tray.

3.4.1. % Of Jet Flood

The flooding condition fixes the upper limit of vapor velocity. Jet flood is caused by massive liquid

entrainment to the tray above due to large vapor velocities. Target for jet flood on sieve trays is between 40% and 82% of jet flood. At 82% of jet flood there is roughly a 99% probability that the tower will operate without jet flooding according correlation (Kister 1992) [1]. At 99% of jet flood there is a 50% probability that the tower will not operate due to jet flood. Below 40% of jet flood the predictions are outside the range of data used to develop the correlation. Past operating experience also suggests possible operational instability below 40% of jet flood.

3.4.2. % Of Down Comer Flood

Down comer flood is caused by not enough down comer open area at the entrance to allow for vapor disengagement, i.e. the entrance velocity is too high. Target for % of down comer (DC) flood is to not exceed 50%, although the method used in this work is the somewhat conservative Glitsch method (Kister 1992) [1]. This method does not consider downcomer backup but rather is looking at the approach to critical downcomer velocities at which point vapors cannot disengage from the liquid entering the downcomer.

3.4.3. % Of Downcomer Backup

Downcomer backup occurs when aerated liquid is backed up in the downcomer due to tray pressure drop, liquid height on the tray and frictional losses in the downcomer apron. Maximum design downcomer backup is 50% of the tray spacing.

3.4.4. Weir Load

Weir loading is an indication of the liquid loading in the tower. High weir loading can result in jet flood. Weir load is calculated as liquid flow rate divided by the length of the outlet weir. Weir load is best below 8 gpm per inch of weir and should not exceed 13 gpm/in to prevent premature flood. Weir load can be reduced by increasing the number of flow paths.

Low weir loading can result in loss of downcomer seals or spray regime. Below 2 gpm/in weir load, seal pans or inlet weirs are required to maintain downcomer seals.

3.4.5. Downcomer Entrance Velocity

The maximum velocity of clear liquid in the downcomer needs to be low enough to prevent chocking and to permit rise and satisfactory disengage-ment of vapor bubbles from the downcomer liquid. This is most restrictive in systems that have a high foaming tendency. DC entrance velocity above 0.5 ft/sec is risk for premature flood. For foaming systems, DC entrance velocity above 0.1 ft/sec is risk for premature flood.

3.4.6. Dry Tray Pressure Drop

For valves trays, dry tray pressure drop below 0.7 in of H_2O is risk for excessive weeping. For sieve trays, the weep fraction estimates are more accurate than for valve trays and should be looked at more than dry tray pressure drop.

3.4.7. Top Downcomer to Tower Area Ratio

The downcomer from a tray must be adequate to carry the liquid flow plus entrained foam and froth. This foamy material is disengaged in the downcomer as only clear liquid flows onto the tray below. A minimum 8% downcomer area is required to prevent premature flooding.

3.4.8. Bottom Downcomer to Tower Area Ratio

A minimum and maximum downcomer area to tower area ratio is required to transfer liquid from top to bottom tray smoothly without flooding.

3.4.9. Flow Path Length

The flow path length (FPL) is the average distance travelled by the liquid leaving one downcomer to the weir of the next adjacent downcomer. If the FPL is too short, part of the liquid will flow into the downcomer without significant contact with the vapor, which will result in a reduction of tray efficiency. Too long FPL can lead to liquid short circuiting and misdistributions.

3.4.10. Weep Fraction

The lower limit of the operating range occurs when liquid leakage through the plate holes becomes excessive. This is known as the weep point. The vapor velocity at the weep point is the minimum value for stable operation. The hole area must be chosen so that at the lowest operating rate the vapor flow velocity is still well above the weep point. (Sinnot1989) [2].

Best practice guidelines for weep fraction are below 0.25. Below 0.25, weeping can occur without significant loss in separation efficiency. For sieve trays the weep fraction results are reasonably accurate and should be consulted for design. For valve trays the weep fraction estimates are more questionable especially for the float valves. As a result, the dry tray pressure drop is better indicator for turndown design.

3.4.11. Entrainment Fraction

As vapor velocities increase, the amount of liquid entrained to the tray above increases. In some cases, the fraction of liquid entrained can be fairly high even though jet flood is not an issue. This creates back mixing and loss of efficiency. Maximum design liquid entrainment fraction is 0.1% of jet flood is generally a better indicator of potential tower performance, but if entrainment fraction exceeds 0.1 while still below 82% of jet flood the engineer should consider the potential impact of entrainment on separation efficiency.

However the values of the above constraints are dependent on the detailed design and very much problem specific. In this work the values of constraints are selected as per general guidelines given by Sinnot (1989) and Kister (1992) [1, 2] and user is not restricted to adhere these values. The value of these constraints must be judiciously selected as they have a big impact on final solution and cost. In case user does not have specific restriction on these values, the constraints should be kept as broad as possible. This will facilitate the lowest cost distillation column.

Attempt has been made in this work to apply PSO optimization technique to design a lowest cost distillation column and satisfy all of the above constraints.

4. HYBRID PARTICLE SWARM AND ANT COLONY OPTIMIZATION: AT A GLANCE

4.1. Particle Swarm Optimization

Particle swarm optimization (PSO) was developed by Kennedy and Eberhart (1995) [4] as a stochastic optimization algorithm based on social simulation models. The algorithm employs a population of search points that moves stochastically in the search space (Shelokar *et al*. 2007) [7]. Concurrently, the best position ever attained by each individual, also called its experience, is retained in memory. This experience is then communicated to part or the whole population, biasing its movement towards the most promising regions detected so far. The communication scheme is determined by a fixed or adaptive social network that plays a crucial role on the convergence properties of the algorithm. The development of PSO was based on concepts and rules that govern socially organized populations in nature, such as bird flocks, fish schools, and animal herds. Unlike the ant colony approach, where stigmergy is the main communication mechanism among individuals through their environment, in such systems communication is rather direct without altering the environment.

4.2. PSO Algorithm

In PSO, candidate solutions of a population, called particles, coexist and evolve simultaneously based on knowledge sharing with neighboring particles. While flying through the problem search space, each particle generates a solution using directed velocity vector. Each particles modifies its velocity to find a better solutions (position) by applying its own flying experience (i.e. memory having best position found in the earlier flights) and experience of neighboring particles (i.e. best found solution of the population). Particles update their positions and velocities as shown below (Shelokar *et al*. 2007) [7]:

$$v_{t+1}^{i} = w_t v_t^{i} + c_1 r_1 \left(p_t^{i} - x_t^{i} \right) + c_2 r_2 \left(p_t^{g} - x_t^{i} \right) \tag{9}$$

$$v_{t+1}^{i} = x_t^{i} + v_{t+1}^{i} \tag{10}$$

Where x_t^i represents the current position of particle i in solution space and subscript t indicates an iteration count p_t^i is the best-found position of particle i up to iteration count t and represents the cognitive contribution to the search velocity v_t^i. Each component of v_t^i can be clamped to the range $\left[-v_{\max}, v_{\max}\right]$ to control excessive roaming of particles outside the search space; p_t^g is the global best-found position among all particles in the swarm up to iteration count t and forms the social contribution to the velocity vector r_1 and r_2 are random numbers uniformly distributed in the interval (0, 1), while c_1 and c_2 are the cognitive and social scaling parameters, respectively; w_t is the particle inertia, which is reduced dynamically to decrease the search area in a gradual fashion. The variable w_t is updated as:

$$W_t = \left(W_{\max} - W_{\min}\right) * \frac{\left(t_{\max} - t_{\min}\right)}{t_{\max}} + W_{\min} \tag{11}$$

Where w_{max} and w_{min} denote the maximum and minimum of w_t respectively. t_{max} are a given number of maximum iterations. Particles i fly toward a new position. In this way, all particles P of the swarm find their positions and apply these new positions to update their individual best p_t^i points and global best p_t^g of the swarm. This process is repeated until iteration count $t = t_{max}$ (a user defined stopping criterion is reached).

4.3. Ant Colony Optimization (ACO)

ACO is a multi-agent approach that simulates the foraging behavior of ants for solving difficult combinatorial optimization problems, such as, the travelling salesman problem and the quadratic assignment problem. Ants are social insects whose behavior is directed more toward the survival of the colony as a whole than that of a single individual of the colony. An important and interesting behavior of an ant colony is its indirect co-operative foraging process. While walking from food sources to the nest and vice versa, ants deposit a substance, called pheromone on the ground and form a pheromone trail. Ants can smell pheromone, when choosing their way, they tend to choose, with high probability, paths marked by strong pheromone concentrations (shorter paths). Also other ants can use pheromone to find the locations of food sources found by their nest mates. In fact, ACO simulates the optimization of ant foraging behavior (Shelokar *et al*. 2007) [7]. Recently there are few adaptations of ACO for solution of continuous optimization problems. Motivated by Dr. Lahiri, Applications of Metaheuristics in Process Engineering, Springer, Switzerland, (2014) [12] in this work, a simple pheromone-guided search mechanism of ant colony is implemented which acts locally to synchronize positions of the particles of PSO to quickly attain the feasible domain of objective function.

4.4. Hybrid PSO and ACO Algorithm

This section describes the implementation of proposed improvement in particle swarm optimization using an ant colony approach. The proposed method (Shelokar *et al*. 2007) [7], called, hybrid particle swarm ant colony optimization (henceforth referred as PSACO) is based on the common characteristics of both PSO and ACO algorithm, like, survival as a swarm (colony) by coexistence and cooperation, individual contribution to food searching by particle (an ant) by sharing information locally and globally in the swarm (colony) between particles (ants), etc. PSACO utilized PSO as a global search and the idea of ant colony approach worked as a local search and updated the positions of the particles by applied pheromone-guided mechanism.

The hybridization of this type of evolutionary algorithm are popular, partly due to its better performance in handling noise, uncertainty vagueness and imprecision. In general there are two important issue in solving global and highly nonconvex optimization problem. These are;

1: Premature convergence – The problem of premature convergence lead to lack of faith of final solution.

2: Slow convergence – This means, the solution quality does not improve sufficiently quickly.

Above two issues can be attributed to the solution diversity that an algorithm can produce in the searching process. In nature, the varsity is maintained by the variety (Quality) and abundance (quantity) of organism at a given place and time. Similarly at the beginning of a search process in PSACO algorithm usually diversity is high and it decreases as the population move towards the global optimum. High diversity in PSO algorithm may provide better guarantee to find the optimal solution with better accuracy, but this will lead to slow convergence, and thus there are some tradeoffs between convergence and accuracy. On the other hand, low diversity may lead to fast convergence while sacrificing the guarantee to find global optimality and with poor solution accuracy. High diversity of PSO algorithm encourages exploration and low diversity does not necessarily mean exploitation because exploitation requires the use of landscape information and the information extracted from the population during the search process. This clever exploitation at the right time and the right place is done by ACO. To enable this hybridization of PSACO algorithm is used to promote diversity and local exploitation along the search for global optimum.

The implementation of PSACO algorithms consists of two stages. In the first stage, it applies PSO while ACO is implemented in the second stage. ACO works as a local search, wherein, ants apply pheromone-guided mechanism to refine the positions found by particles in the PSO stage. In PSACO a simple pheromone-guided mechanism of ACO is proposed to apply as local search (Shelokar *et al*. 2007) [7]. The proposed ACO algorithm handles P ants equal to the number of particles in PSO. Each ant i generate a solution z_t^i around p_t^g the global best-found position among all particles in the swarm up to iteration count as;

$$z_t^i = \mathrm{N}\left(p_t^g, \sigma\right) \tag{12}$$

In eq. 12 we generate components of solution vector z_t^i which satisfy Gaussian distributions with mean p_t^g and standard deviation σ, where, initially at t=1 value of σ=1 and is updated at the end of each

Table 3: Pseudo Code for Hybrid PSO and ACO Algorithm

Step 1.	Initialize optimization
Step 1.1.	Initialize constants for PSO and ACO algorithm t_{max}, P
Step 1.2.	Initialize randomly all particles positions x_t^i and velocities v_t^i
Step 1.3.	Evaluate objective function values as $f\left(x_t^i\right)$
Step 1.4.	Assign best positions $p_t^i = x_t^i$ with $f\left(p_t^i\right) = f\left(x_t^i\right), i = 1,...,P$
Step 1.5.	Find $f_t^{best}\left(p_t^{best}\right) = \min\left\{f\left(p_t^1\right),...,f\left(p_t^i\right),..,f\left(p_t^P\right)\right\}$ And initialize $\left(p_t^g\right) = p_t^{best} and\ f\left(p_t^g\right) = f_t^{best}\left(p_t^{best}\right)$.
Step 2.	Perform optimization While $\left(t \le t_{max}\right)$
Step 2.1.	Update particle positions x_t^i and velocities v_t^i according to equations (6.24) and (6.25) of all P particles.
Step 2.2.	Evaluate objective function value as $f\left(x_t^i\right)$
Step 2.3.	Generate P solutions z_t^i using equation (6.26)
Step 2.4.	Evaluate objective function value as $f\left(z_t^i\right)$ and if $f\left(z_t^i\right) < f\left(x_t^i\right)$ then $f\left(x_t^i\right) = f\left(z_t^i\right)$ and $x_t^i = z_t^i$.
Step 2.5.	Update particle best position if $f\left(p_t^i\right) > f\left(x_t^i\right)$ then $p_t^i = x_t^i$ with $f\left(p_t^i\right) = f\left(x_t^i\right),\ \ i = 1,...,P$.
Step 2.6.	Find $f_t^{best}\left(p_t^{best}\right) = \min\left\{f\left(p_t^1\right),...,f\left(p_t^i\right),..,f\left(p_t^P\right)\right\}$
If $f\left(p_t^g\right) > f\left(p_t^{best}\right) then\ p_t^g = p_t^{best} and\ f\left(p_t^g\right) = f^{best}\left(p_t^{best}\right)$.	
Step 2.7.	Increment iteration count t = t+1.
End while	
Step 3.	Report best solution p^g of the swarm with objective function value $f(p^g)$.

iteration as σ = σ*d, where, d is a parameter in (0.25, 0.997) and if σ < σ_{min} then σ = σ_{min} where σ_{min} is a parameter in (10^{-2}, 10^{-4}). Compute objective function value f(z_t^i) using z_t^i and replace position x_t^i the current position of particle i in the swarm if f(z_t^i) < f(x_t^i) as x_t^i = z_t^i and f(x_t^i) = f(z_t^i). This simple pheromone-guided mechanism considers, there is highest density of trails (single pheromone spot) at the global best solution p_t^g of the swarm at any iteration t in each stage of ACO implementation and all ants P search for better solutions in the neighborhood of the global best solution. In the beginning of the search process, ants explore larger search area in the neighborhood of p_t^g due to the high value of standard deviation σ and intensify the search around p_t^g as the algorithm progresses. Thus, ACO helps PSO process not only to efficiently perform global exploration for rapidly attaining the feasible solution space but also to effectively reach optimal or near optimal solution.

The pseudo-code of PSACO method is given in Table **3** (Shelokar *et al*. 2007)[7] where P denotes the number of particles in the population; f(x_t^i) represents the objective function value of particle i at position x, while $f_t^{best}\left(x_t^{best}\right)$ represents the best function value in the population of solutions P at iteration count t.

The algorithm starts with initializing parameters of both PSO and ACO methods. The first stage consists of PSO, which generates P solutions.

Objective function values are computed as f(x_t^i). ACO is applied in the second stage to update the positions of particles in the swarm. This process is repeated until iteration count t = tmax.

4.5. Handling the Constraints

The original problem can be set as,

$$\text{Minimize } C_{tot}(x)$$

$$\text{Subject to } g_i(x) \le 0 \text{ where } i = 1, 2,\ldots,m$$

Where x is the vector of optimization variables. The set of constraints g(x) corresponds to the inequalities.

For implementation of the PSO algorithm, we used a penalty function in the objective function, to provide the following objective function to be minimized. (Ponce Ortega *et al*. 2009)[13].

$$\text{Obj}(x) = C_{tot}(x) + \text{penalty}(x) \quad (13)$$

The penalty function accounts for the violation of the constraints such that:

$$penalty(x) = \begin{cases} 0 & if\ x\ is\ feasible \\ \sum_{i=1}^{m} r_i g_i^2(x) & otherwise \end{cases} \quad (14)$$

Where r_i a variable penalty coefficient for the ith constraint is, r_i varies according to the level of violation. To provide an efficient algorithm, the value of each, r_i was increased proportionally as a function of the number of generations.

5. SIMULATION AND PSACO IMPLEMENTATION

5.1. Process Simulation

Simple process simulation of distillation problem stated above was done in commercial simulators (Aspen plus). As a base case simulation, total number of stages is fixed at 29 and feed tray location is fixed at 11. Reflux ratio and reboiler heat duty were varied to meet the product purity specification. Same procedure is repeated for total plate number 10 to 35 and some of

Table 4: Simulation Results

Stage	Feed Stage	Liquid Mass Flow Rate	Vapor Mass Flow Rate	Liquid Density	Vapor Density	Liquid Viscosity	Vapor Viscosity	Surface Tension	Reboiler heat duty	Condenser heat duty
		kg/sec	kg/sec	kg/m^3	kg/m^3	cP	cP	dyne/cm	MW	MW
24	11	30.41	18.65	542.51	18.07	0.13	0.01	6.95	5.61	4.95
25	11	30.41	18.64	542.51	18.07	0.13	0.01	6.95	5.61	4.95
26	12	30.40	18.63	542.51	18.07	0.13	0.01	6.95	5.61	4.95
27	12	30.40	18.63	542.51	18.07	0.13	0.01	6.95	5.61	4.95
28	13	30.39	18.63	542.51	18.07	0.13	0.01	6.95	5.61	4.95
29	13	30.39	18.63	542.51	18.07	0.13	0.01	6.95	5.61	4.95
30	14	30.39	18.63	542.51	18.07	0.13	0.01	6.95	5.61	4.95
31	14	30.39	18.63	542.51	18.07	0.13	0.01	6.95	5.61	4.95
32	15	30.39	18.63	542.51	18.07	0.13	0.01	6.95	5.61	4.95
33	15	30.39	18.63	542.51	18.07	0.13	0.01	6.95	5.61	4.95
34	16	30.39	18.62	542.51	18.07	0.13	0.01	6.95	5.61	4.95
35	16	30.39	18.62	542.51	18.07	0.13	0.01	6.95	5.61	4.95

Table 5: Simulation Results for Different Feed Tray Location

Stage	Feed Stage	Liquid Mass Flow Rate	Vapor Mass Flow Rate	Liquid Density	Vapor Density	Liquid Viscosity	Vapor Viscosity	Surface Tension	Reboiler Heat Duty	Condenser Heat Duty
		kg/sec	kg/sec	kg/m^3	kg/m^3	cP	cP	dyne/cm	MW	MW
29	8	30.58	18.80	542.59	18.07	0.13	0.01	6.96	5.66	5.01
29	9	30.48	18.71	542.58	18.07	0.13	0.01	6.95	5.63	4.98
29	10	30.44	18.67	542.58	18.07	0.13	0.01	6.95	5.62	4.97
29	11	30.41	18.65	542.58	18.07	0.13	0.01	6.95	5.61	4.96
29	12	30.40	18.64	542.58	18.07	0.13	0.01	6.95	5.61	4.96
29	13	30.40	18.63	542.58	18.07	0.13	0.01	6.95	5.61	4.96
29	14	30.40	18.63	542.58	18.07	0.13	0.01	6.95	5.61	4.96
29	15	30.40	18.63	542.58	18.07	0.13	0.01	6.95	5.61	4.96
29	16	30.40	18.63	542.58	18.07	0.13	0.01	6.95	5.61	4.96
29	17	30.40	18.64	542.58	18.07	0.13	0.01	6.95	5.61	4.96
29	18	30.42	18.65	542.58	18.07	0.13	0.01	6.95	5.61	4.96
29	19	30.45	18.68	542.58	18.07	0.13	0.01	6.95	5.62	4.97

the results are tabulated in Table **4**. For the same total number of stages, different feed tray location was tested as sensitivity analysis and results were partly shown in Table **4** for sake of brevity. The whole results similar to Table **5** were exported as matrix in Matlab which was later used by PSACO algorithm during optimization.

5.2. PSACO Implementation

PSACO Code was developed in Matlab environment. The algorithm begins generating a set of random initial populations, that is, a set of values within their bounds for the nineteen optimization variables (refer Table **1**) according to the population sizes. Each of these individuals (set of design or search variables) is then fed to the design algorithm for distillation column to obtain a set of constraints (using equations 15-108 in Appendix 1) and total annual cost (using equations 1-8 stated above). Based on the randomly selected total number of stages and feed tray location, the appropriate value for reboiler and condenser duty, maximum vapor and liquid load were selected and used in the hydraulic calculations and objective function evaluations. The fitness function i.e. total cost (equation 1) for each individual of the population is evaluated depending upon their violation of constraints. From those values, the algorithm (Appendix 2) selects the best individuals of the current generations as the parents to new generations. The procedure is repeated until the optimal design or lowest total cost detected. The objective function is the minimization of PTDC total cost given in equation 1 and x is a solution string representing a design configuration. The algorithm stopped when no further improvement in the fitness function in 30 successive generations was observed. As an alternative termination step, a maximum of 300 generations was imposed.

In the present study, the product purity and hydraulic constraints (given in Table **2**) is considered to be the feasibility constraint. For a given design configuration, whenever any of the above constraints exceeds the specified limit, an infeasible configuration is returned through the algorithm so that as a low priority configuration it will be gradually eliminated in the next iteration of the optimization routine.

6. RESULTS AND ANALYSIS

The effectiveness of the present approach using PSACO algorithm is assessed by analyzing case study. The case study was analyzed using traditional optimization approach available in commercial simulators (Aspen plus) and taken from literature (Filipe Soares Pinto, Roger Zemp, Megan Jobson, Robin Smith, 2011) [11].

The original design specifications, shown in Table **1**, are supplied as inputs along with their upper and lower bounds to the described PSACO algorithm. These upper and lower bounds are taken as per broad guidelines given by Kister (1992) & Sinnot (1989) [1, 2].

PSACO algorithm was run for 100 times with different random initial seeds.

If the PSACO is applied in straight forward manner, it is seen that column diameter was chosen randomly and most of the time selected small diameter cannot handle liquid and vapor load and ended up with high value of jet flooding or downcomer flooding. So, choosing the diameter randomly leads to infeasible solution and waste computational time to arrive at feasible solution. To avoid this trap, a simple methodology is used, where column diameter was back calculated corresponds to 80% flooding for a given vapor and liquid load. This diameter was then set as a minimum column diameter (d_{min}) in Table **1**. This trick improves the number of feasible solution and computational time significantly.

Table **6** gives the different solutions found by applying PSACO along with corresponding cost. Table **7** gives the corresponding value of the constraints.

Following points are noteworthy from the results of Table **6** and **7**.

6.1. Multiple Optimum Solutions

Instead of a single optimum solution, this work generates multiple optimum solutions. For sake of brevity, 10 such best solutions are tabulated in Table **6** and corresponding constraints are given in Table **7**. From Table **6** and **7**, it is clear that multiple distillation column configuration is possible with practically same cost or with little cost difference. All these solutions are feasible and user has flexibility to choose any one of them based on his requirement and engineering judgment.

The lowest total cost is found 0.867M$(corresponds to solution number 1 in Table **6**) and all other solutions are within 50% cost of global minimum cost. From Table **6**, it is found that all constraints are well within

Table 6: Optimal Column Geometry Using Improved PSACO Methods

Variable Notation	1	2	3	4	5	6	7	8	9	10
d_t	2.26	2.19	2.13	2.37	2.20	2.23	2.62	2.58	3.30	3.05
tray space	0.66	0.73	0.84	0.56	0.74	0.83	0.84	0.65	0.49	0.85
vtype	0.00	0.00	0.00	0.00	0.00	0.00	0.00	0.00	0.00	0.00
ϕ	0.14	0.14	0.14	0.15	0.15	0.15	0.14	0.15	0.13	0.14
d_h	0.0033	0.0041	0.0032	0.0045	0.0033	0.0119	0.0033	0.0045	0.0064	0.0060
$deck_t$	0.0060	0.0054	0.0062	0.0037	0.0061	0.0050	0.0061	0.0061	0.0012	0.0017
passcfg	0.0342	0.0375	0.0329	0.0360	0.0308	0.0327	0.0345	0.0351	0.0329	0.0359
h_w	0.0381	0.0381	0.0381	0.0381	0.0381	0.0381	0.0381	0.0381	0.0381	0.0381
w_{dct}	0.36	0.38	0.35	0.36	0.36	0.35	0.38	0.43	0.43	0.43
w_{dcb}	0.35	0.36	0.34	0.35	0.35	0.38	0.41	0.39	0.35	0.35
w_{dcs}	0.0000	0.0000	0.0000	0.0000	0.0000	0.0000	0.0000	0.0000	0.0000	0.0000
c_{dc}	0.0762	0.0754	0.0742	0.0759	0.0759	0.0748	0.0758	0.0742	0.0745	0.0762
ch_w	0.0393	0.0500	0.0598	0.0862	0.0853	0.0539	0.0595	0.0726	0.0440	0.0818
w_{cdct}	0.44	0.45	0.38	0.43	0.49	0.42	0.46	0.4	0.41	0.34
w_{cdcb}	0.68	0.95	1.12	0.92	0.68	1.02	0.78	0.91	1.15	1
w_{cdcs}	0.0000	0.0000	0.0000	0.0000	0.0000	0.0000	0.0000	0.0000	0.0000	0.0000
c_w	0.0502	0.0676	0.0551	0.0673	0.0467	0.0521	0.0346	0.0631	0.0382	0.0440
stgno	18	21	21	22	23	23	16	17	28	19
feedstg	15	14	14	11	12	13	13	9	8	9
C_E	0.568	0.568	0.568	0.595	0.582	0.572	0.676	0.733	0.676	0.841
C_{cap}	0.898	0.966	0.997	0.943	1.008	1.054	1.040	0.999	1.180	1.270
C_{tot}	0.867	0.890	0.900	0.910	0.918	0.923	1.022	1.066	1.069	1.264

their upper and lower limits and thus represent a feasible solution. If someone looks in detail into the various solutions of Table **5**, he will be amazed the variety of solutions with different height, diameter of column and different feed stage locations. Now, users have the flexibility to choose any of these solutions based on his engineering judgment. Note that, in actual shop floor, lowest cost design may not be always the best design.

6.2. Analysis of Minimum Cost Design

Corresponding to minimum cost design, column diameter is 2.26Meter, plates are 2B pass configuration, total number of stage is 18 with feed stage 15(refer Table **6**). Energy and capital cost are 0.568 and 0.898 M$ respectively. As seen from Table **7** none of the constraints hits their limit. However, jet flood% is 78.53% against 80% maximum limit. The

Table 7: Value of Constraints Corresponding to Optimum Solution

Constraints	1	2	3	4	5	6	7	8	9	10
%Jet flood	78.53	78.41	77.33	76.72	76.41	78.83	72.48	50.51	63.55	52.03
%Downcomer flood	44.89	47.70	47.78	47.54	46.77	45.94	45.52	39.60	47.63	42.91
%Downcomer Back up	16.42	18.25	14.46	19.94	15.31	14.82	17.88	21.07	13.84	13.89
weir load	2.22	2.44	2.38	2.33	2.39	2.29	2.96	2.00	3.21	3.15
u_{ldc}	0.08	0.09	0.10	0.08	0.09	0.09	0.08	0.04	0.10	0.07
dp	344.74	344.74	344.74	275.79	344.74	344.74	344.74	275.79	275.79	344.74
ar_{dct}	9.36	8.65	8.15	8.61	8.62	8.41	11.39	11.13	9.35	11.37
FPL	1.55	1.63	1.55	1.71	1.59	1.59	1.73	2.29	1.81	2.11
w_{frac}	0.04	0.07	0.06	0.14	0.12	0.00	0.14	0.25	0.19	0.14
e_{frac}	0.0088	0.0096	0.0042	0.0100	0.0039	0.0116	0.0012	0.0001	0.0000	0.0000

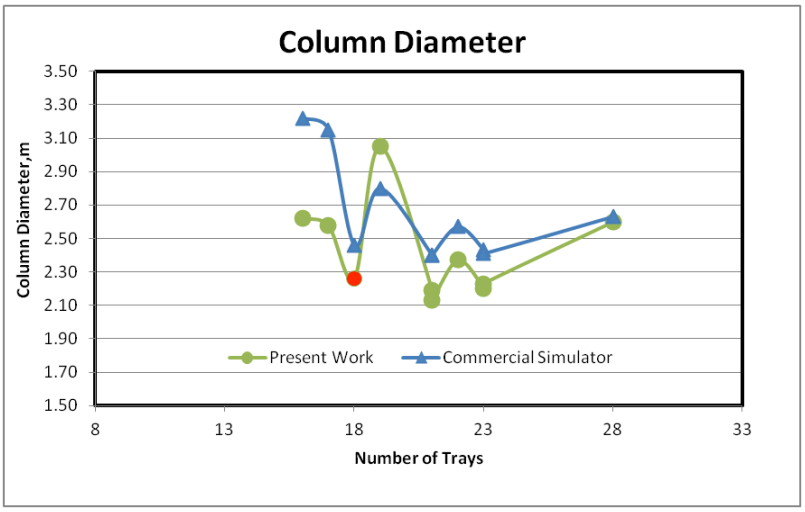

Figure 2: Column diameter at different number of stages (Commercial simulator vs. present work).

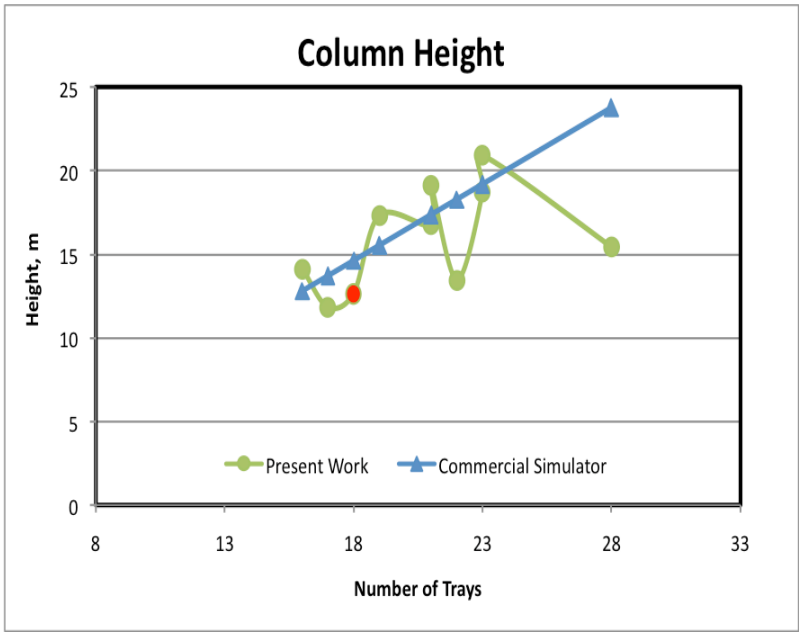

Figure 3: Column height at different number of stages (Commercial simulator vs. present work).

following design variables hits their limit: Outlet weir height hits it minimum value of 0.0381m, Hole area (fraction of bubbling area) hits at maximum value of 0.15, Downcomer clearance hits at maximum value of 0.0762 (refer Table **6**) which indirectly indicates that relaxing any of their limit may reduce total cost further. User need to investigate that whether he has the scope/flexibility to relax their limits of the above variable further.

The jet flood 78.53% and downcomer backup 16.42% are well within their limit. From energy and capital cost value of 10 solutions tabulated in Table **6**, it is concluded that energy cost is the dominant factor (corresponds to 66% of total cost) as compared to capital investment in the optimum solutions. Note that a payback period of 3 years was taken to calculate the total cost as per equation 1.

6.3. Comparisons of Results with Commercial Simulators

The resulting optimal columns architectures obtained by PSACO are compared with the results obtained from commercial simulators and shown in Figure **2-4**. Aspen plus simulation model is used to compare the result. As stated earlier, for each total number of stages, sensitivity analysis was carried out in commercial simulator by varying feed stage location. The feed stage which corresponds to minimum total

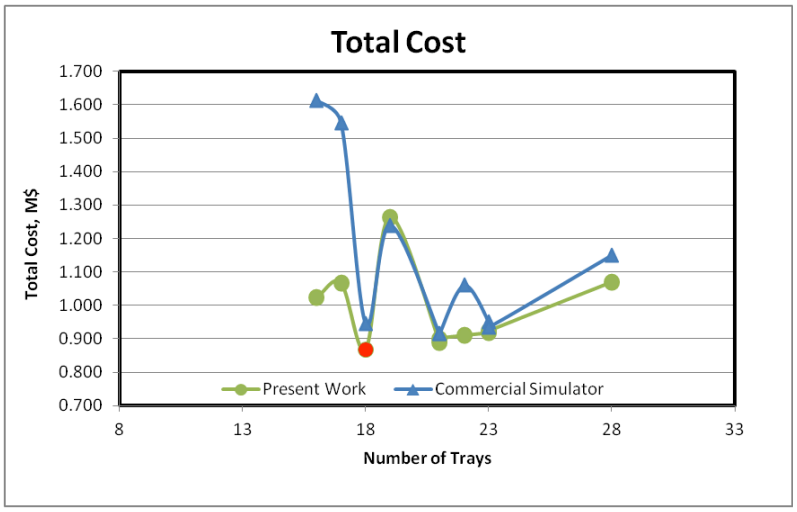

Figure 4: Total cost at different number of stages (Commercial simulator vs. present work).

cost of the column is taken as reference feed stage to draw the plot of Figure **2-4**. Different hydraulic parameter input in aspen simulation model like tray spacing, hole diameter etc… are kept at default value due to absence of guidelines for this particular problem. As seen from these figures, column diameter, column height and overall total cost are less in the present work as compared to results obtained from commercial simulators. The red color candidate in Figure **2-4** corresponds to global best solution as indicated in first column of Table **6**. This is possible due to optimum selection of various tray geometric parameters like fractional hole area, hole diameter, downcomer width, tray spacing weir height etc. Optimum values of these parameters (refer Table **6**) helps to reduce the capital and total cost of the column. On the contrary, in commercial simulators, most of the time these parameters are treated as user input and designer gives these parameters as default value or based on his experience. This proves a genuine advantage of applying PSACO in PTDC design.

6.4. Advantages of PSACO over Standard PSO

As seen from literature standard PSO has been applied mainly for unconstrained continuous optimization problems. The application of standard PSO in the field of constrained optimization problem is very few.

When standard PSO (without ACO) with penalty function method is applied at current PTDC design problem, it was found that most of the time the algorithm unable to find a feasible solution. This is due to very complex nonlinear relationship of constraints (like flooding, downcomer flooding, weeping, entrainment, pressure drop etc.) with the search optimization variables (like column diameter, tray spacing, downcomer width etc.). After large number of trials with extensive computational effort, such algorithm sometimes able to find out feasible solutions but the final solution are much inferior as compared to solutions of PSACO.

On the contrary, when PSACO was applied in current case study, the execution time to arrive at lowest cost feasible solution increase dramatically. The solution space of PTDC cost is very noisy and complex and having lot of minima. Considering the feasibility based rule tends to cause high pressure of feasibility on the particles, hybrid algorithm combining PSO and ACO helps to overcome the premature convergence. In particular, the property of ACO is employed to the best of the swarm to help PSO escape from local optima. This is evident from the fact that, in present case study, out of 100 fresh starts, most of the time algorithm converges to global minima. Also each time it is able to converge to feasible solution. The quality of final solution is better than standard PSO and number of function evaluations and execution time is much less than standard PSO. In a standard pentium4 processor execution time is 1.4hrs and 0.5hrs. Respectively for PSO and PSACO algorithm. Based on the simulation results and comparisons, it can be concluded that the present algorithm is of superior searching quality and robustness for constrained engineering design problems.

Other distinct advantages of present approach over traditional approach of PTDC design are explained below:

6.5. Integrated Approach to Determine the Number of Equilibrium Stage and Column Diameter

In this work, number of equilibrium stage and diameter of column is determined by the method of overall total cost minimization. In traditional technique of chemical engineering, most of the time they are determined by equilibrium calculation and hydraulic calculation separately. As reflux ratio has great influence on both of them, these two calculations are intermingled and cannot be separated. In present technique, its influence on total cost is analyzed simultaneously and number of equilibrium stage and diameter of column is determined by the method of overall total cost minimization technique.

7. STRATEGY TO SELECT TRAY GEOMETRIC PARAMETERS

This method provides a strategy to intelligently determine the value of various tray geometric parameters like tray spacing, downcomer width, sieve hole diameter, weir height etc. Traditionally these parameters are determined by experience or by some heuristic guidelines. Most of the time, these parameters were not changed e.g. tray spacing was traditionally kept 24 inch in most of the column design. These parameters had very important impact on column design and had immense influence on column cost. As for example, low tray spacing reduces the capital cost by reducing column height, whereas increase the cost by increase the column diameter. Hence their appropriate value should be judiciously selected by optimizing the column overall cost. This methodology gives a platform to select these tray geometric parameters by minimizing column cost while obeying all the hydraulic constraints like flooding, entrainment, pressure drop etc. However, if for any special case, designer want to fix the value of any of these parameters based on his special consideration/ experiences, he can freely able to do so by putting same upper and lower limit in Table **4**. This algorithm will not change the value of that particular parameter in course of optimization.

7.1. Detail Hydraulic Calculation

Commercial simulators like aspen plus, ProII does not perform detail tray hydraulic calculation as implemented in this work. Most of the cases, tray vendors like Koch glitch, Sulzer had their proprietary software to perform detail hydraulic calculations. These softwares are available as executable files and cannot perform the iterative calculations. The detail engineering designer, usually perform the equilibrium calculations in commercial simulators (like aspen plus, Hysys, ProII etc.) to determine number of stages and then export the tray loading variables to tray vendor software (like Sulzer software) to perform the hydraulic calculations to determine the column diameter. Most of the cases, total cost is ignored in this type of functional design stages. Also, once through calculations do not necessarily leads to most cost effective design. This work, gives a platform to optimize all the parameters by performing an iterative detail hydraulic calculations and optimize them simultaneously.

7.2. Optimize Feed Tray Location

This work gives a methodology to select feed stage location. Strategy adopted here is simple: feed stage should be located in such a tray where overall cost should be minimum. This is quite different from the traditional feed stage location procedure where feed was introduced to a tray where liquid / vapor compositions matches with feed composition. Actually, location of feed tray greatly influences the reboiler/condenser duty, liquid and vapor traffic in the column. In other words, feed tray location has a big impact on column working capital (energy cost) and initial investment cost. So where cost minimization is the main design objective, the best strategy is to locate the feed tray in such position which corresponds to overall total minimum cost.

7.3. Choosing Best Design Configurations from Various Alternatives of Columns

The solution space of cost objective function with multiple constraints is very much complicated with multiple local minima. Cost wise these local minima may be very near to each other but geometrically represent complete different sets of columns. To assess these multiple local minima, the PSACO program was run 100 times with new starting guess every time. Most of the times PSACO converged to global minima but sometimes it were found that it got stuck to local minima depending upon the complexity of solution space. All these feasible solutions were collected and solution within 50% of global minimum cost is presented in Table **6** for case study. From this table, it is clear that multiple distillation column configuration is possible with practically same cost or with little cost difference. All these solutions are feasible and user has flexibility to choose any one of them based on his requirement and engineering

judgment. As for example, some user has very less space available in his company, so he may choose lowest diameter column. Selecting the best distillation design from Table **6** is a combination of science and arts. Decision of best column selection for a particular service and industry is based on multiple criteria including costs. Criteria like maintainability, ease of cleaning, flow induced vibrations; less floor space requirement, compactness of design etc…sometimes influence the best selection decision much more than the simple lowest cost criteria. The lowest cost column is not always performing best in actual shop floor. These criteria though very influential for final selection of column are often qualitative and difficult to express quantitatively. Sinnot (1989) [2] gives some broad guidelines regarding various criteria influence the final choice. It requires designer experience, engineering judgment, customer requirements and normally very problem specific. By default, the first solution in Table **6** is considered as the best column as this represents the lowest cost column which satisfies all the constraints. Then users have to compare the first solution with the other solutions in Table **6** one by one and based on his specific requirements, the best column to be found out. All the solutions in Table **6** are within 50% range of lowest cost column (i.e. their costs are comparable) and users can select the best for his service from variety of solutions. The final decision is dedicated to the user.

CONCLUSION

Plate type distillation column design can be a complex task and advanced optimization tools are useful to identify the best and cheapest column for a specific separation. The present study has demonstrated successful application of PSACO technique for the optimal design of PTDC from economic point of view. This paper has applied hybrid particle swarm Ant colony optimization, which provides an effective alternative for solving constrained optimization problems to overcome the weakness of penalty function methods. The presented PSACO technique is simple in concept, few in parameters and easy for implementations. These features boost the applicability of the PSACO particularly in separation system design, where the problems are usually complex and have a large number of variables and complex nonlinear constraints in the objective function. Furthermore, the PSACO algorithm allows for rapid feasible solutions of the design problems and enables to examine a number of alternative solutions of good quality, giving the designer more degrees of freedom in the final choice with respect to traditional methods. This paper evolve a strategy to optimize various tray geometric parameters like tray diameter, hole diameter, fractional whole area, down comer width etc… and also decide on optimum feed tray location based on overall cost minimization concept. The solutions to case studies taken from literature show how commercial simulator designs can be improved through the use of the approach presented in this work.

NOMENCLATURE

C_{tot} = Total cost (10^6 \$).

C_{cap} = Capital investment (10^6 \$).

C_e = Energy cost (10^6 \$).

C_{col} = Column capital cost (10^6 \$).

C_{HE} = Reboiler and condenser capital cost (10^6 \$).

N_{stage} = Total number of stages (-).

S_{tray} = Tray spacing (m).

$Area_{Reboiler}$ = Reboiler Area (m^2).

$Area_{condenser}$ = Condenser Area (m^2).

C_{steam} = Unit cost of steam (\$/MT).

$Q_{condenser}$ = Condenser heat duty (MW).

U = Total heat Coefficient (W/m^2 K).

Δt = Delta Temperature.

$Q_{Reboiler}$ = Reboiler heat duty (MW).

d_{min} = Minimum diameter (m).

r_1 and r_2 = Random numbers between 0 and 1.

c_1 and c_2 = Cognitive and social scaling parameters.

w_t = Particle inertia.

t_{max} = Given number of maximum iterations.

K = Boltzmann constant.

ε = Step size.

u_{dfc} = Critical froth velocity (m/s).

σ = Surface tension, dynes/cm.

ρ_L = Liquid density, kg/m^3.

ρ_V = Vapor density, kg/m^3.

μ_L = Liquid viscosity, cap.

M_L = Liquid mass flow rate, kg/sec.

q_w = Weep rate (gpm).

q_{ldc} = Liquid rate to downcomer (gpm).

q_L = Liquid rate down tower (gpm).

a_t = Superficial tower area (m^2).

r = Tower radius (m).

d_t = Tower diameter (m).

l_w = Outlet weir length (m).

w_{dct} = Top downcomer (DC) width (m).

a_{dct} = Area downcomer at top (m^2).

l_{dcb} = Bottom downcomer chord length (m).

w_{dcb} = Bottom downcomer (DC) width (m).

a_{dcb} = Area downcomer at bottom (m^2).

l_{dcs} = Bottom downcomer sump chord length (m).

w_{dcs} = Downcomer (DC) sump width (m).

a_{dcs} = Area of bottom downcomer sump (m^2).

a_{dc} = Average downcomer area (m^2).

l_{cdct} = Top centre downcomer chord length (m).

w_{cdct} = Top centre downcomer (DC) width (m).

a_{cdct} = Area of centre downcomer at top (m^2).

l_{cdcb} = Bottom centre downcomer chord length (m).

w_{cdcb} = Bottom centre downcomer (DC) width (m).

l_{cdcs} = Side centre downcomer chord length (m).

w_{cdcs} = Side centre downcomer (DC) width (m).

a_b = Bubbling area (m^2).

h_w = Outlet weir height (m).

ch_w = Centre outlet weir height (m).

u_{bdcvt} = Ub at downcomer critical velocity at downcomer entrance (m/s).

u_{bdcvw} = Ub at downcomer critical velocity within downcomer (m/s).

u_{bdcv} = Bubbling area vapor velocity at dc critical velocity (m/s).

u_b = Vapor velocity based on bubbling area (m/s).

M_V = Vapor mass flow rate, kg/sec.

q_{ls} = Scaled liquid rate down tower for constant l/v (gpm).

F_r = Froude number based on bubbling area.

h_{cl} = Liquid head on tray (m liquid).

η = Volumetric ratio of vapor/liquid on tray.

α_t = Average liquid volume fraction on tray.

h_f = Froth height on tray (m liquid).

C_d = Liquid head coefficient.

h_{cl} = Liquid head on tray (m liquid).

ΔP = Total tray pressure drop (m liquid).

φ = Hole area (fraction of bubbling area).

a_h = Hole area (m^2).

a_b = Bubbling area (m^2).

$weep_{df}$ = Weeping driving force.

u_{BWP} = Weep point (m/s).

$deck_t$ = Deck thickness, m.

d_h = Hole diameter, m.

q_w = Weep rate (gpm).

q_{ldc} = Liquid rate to downcomer (gpm).

a_f = Free area (m^2).

c_b = Capacity factor based on bubbling area (m/s).

c_{bfl} = Capacity factor based on bubbling area at constant liquid rate jet flood (m/s).

u_{lv} = Vertical liquid velocity based on tower area (m/s).

c_s = Capacity factor based on tower area (m/s).

c_{sp} = System limit parameter.

c_{ss} = Capacity factor at system limit based on tower area (m/s).

p_{vsl} = Percent of vapor system limit at constant l/v (%).

v_{load} = Glitch method Vload term (m^3/s).

T_k = Temperature at generation k, C.

FPL = Flow path length (m).

gmpjf = Glitsch method percent jet flood (%).

FID = Flow into the downcomer (gpm/ft^2).

HLUDC = Glitsch method head loss under downcomer (m liquid).

Weir load = Weir loading (gpm/in weir).

DCBU = Glitsch method DC backup (m liquid).

%Jet flood = Final percent of jet flood by most appropriate method.

%Downcomer flood = Glitsch method percent downcomer flood (%).

%Downcomer backup = Glitch method DC backup % of tray spacing (%).

APPENDIX-1

This section describes step by step procedure for calculating various constraints given in Table **2**. The equations are taken from various literatures namely Kister 1992 [1], Sinnot 1989 [2], Lahiri SK [12], Luyben [3] etc. As most of the correlations, plots, monographs and equations found in literature are in FPS unit, the whole calculations (equation 15 to 108) are done in FPS unit and appropriate conversion was made at initial input and final results to convert it to SI unit.

Step 1: Critical froth velocity (ft. /s), (Refer equation 15 in Table **8**)

Step 2: Calculate q_{ldc} −liquid rate to downcomer (gpm) (Refer equation 16 to 18 in Table **8**)

Step 3: Calculate a_{dc} −average downcomer area (ft2) (Refer equation 19 to 32 in Table **8**)

For pass = 2A (Refer equation 33 to 37 in Table **8**)

For pass = 2B (Refer equation 38 to 45 in Table **8**)

For pass = 1 (Refer equation 46 to 47 in Table **8**)

Step 4: Calculate u_{bdcv} -bubbling area vapor velocity at downcomer critical velocity (Refer equation 48 to 50 in Table **8**)

Assume initial hcl = 0.75 inch.

Flag = True

Do while flag = True and iteration<1000

Step 5: Scale q_l for constant l/v

(Refer equation 51 to 52 in Table **8**)

Step 6: Calculate Froude number (Refer equation 53 in Table **8**)

Step 7: Calculate η –vapor/liquid volume ratio on tray (Refer equation 54 in Table **8**)

Step 8: Calculate α_t -liquid volume fraction on tray (Refer equation 55in Table **8**)

Step 9: Calculate h_f -froth height on tray (Refer equation 56 in Table **8**)

Step 10: Calculate C_d -liquid head co-efficient (Refer equation 57 in Table **8**)

Step 11: Calculate h_{cl} -liq head on tray (m liquid) (Refer equation 58 in Table **8**)

Step 12: Calculate ΔP -pressure drop in liquid (Refer equation 59 in Table **8**)

Step 13: Calculate u_l- horizontal liquid velocity (ft/s) (Refer equation 60 to 62 in Table **8**)

Step 14: Calculate $weep_{df}$ −weeping driving force (Refer equation 63 in Table **8**)

Step 15: Calculate q_w.-weep rate (gpm) (Refer equation 64 to 69 in Table **8**)

Step 16: Calculate u_{bdcv}– bubbling area vap velocity at down comer critical velocity (Refer equation 70 to 73 in Table **8**)

If (abs (u_{bdcv1}-u_{bdcv2})<control Or iter ≥ maxiter T hen (Refer equation 74 in Table **8**)

Flag = false

Else,

Calculate from equation 75 and 76 in Table **8**.

Iter = iter+1

Endif

loop

Step 17: Calculate % jet flood by FRI method (Refer equation 77 to 84 in Table **8**)

Step 18: Calculate % jet flood, %DC flood and %DC backup by Glitsch method (Refer equation 85 to 97 in Table **8**)

Step 19: Calculate final constraints values (Refer equation 98 to 103 in Table **8**)

Step 20: Calculate entrainment fraction (Refer equation 104 to 108 in Table **8**).

Table 8: Equations to Calculate Various Constraints of Distillation Column

Equation No.	Equation
Eq. 15	$U_{dfc} = \left[\frac{3.077\sigma^{0.6}(\rho_L - \rho_V)^{0.4}}{\mu_L^{0.2}\rho_L^{0.8}}\right]^{0.556}$
Eq. 16	$q_L = \frac{481M_L}{60\rho_L}$
Eq. 17	$q_L = \frac{481M_L}{60\rho_L}$
Eq. 18	$q_{ldc} = q_L - q_w$
Eq. 19	$a_t = \frac{3.14d_t^2}{4}$

Eq. 20	$r = \frac{12 d_t}{2}$
Eq. 21	$l_w = 2\left[2 w_{dct} r - w_{dct}^2\right]^{0.5}$
Eq. 22	$a_{dct} = \frac{1}{144}\left[\left(\sin^{-1}\frac{l_w}{2r}\right) r^2 - (r - w_{dct})\frac{l_w}{2}\right]$
Eq. 23	$l_{dcb} = 2\left[2 w_{dcb} r - w_{dcb}^2\right]^{0.5}$
Eq. 24	$a_{dcb} = \frac{1}{144}\left[\left(\sin^{-1}\frac{l_{dcb}}{2r}\right) r^2 - (r - w_{dcb})\frac{l_{dcb}}{2}\right]$
Eq. 25	$l_{dcs} = 2\left[2 w_{dcs} r - w_{dcs}^2\right]^{0.5}$
Eq. 26	$a_{dcs} = \frac{1}{144}\left[\left(\sin^{-1}\frac{l_{dcs}}{2r}\right) r^2 - \left(\frac{r - w_{dcs}}{l_{dcs}/2}\right)\right]$
Eq. 27	$l_{cdct} = 2[2\left(r - \frac{w_{cdct}}{2}\right) r - \left(r - \frac{w_{cdct}}{2}\right)^2]^{0.5}$
Eq. 28	$a_{cdct} = a_t - \frac{2}{144}\left[\left(\sin^{-1}\frac{l_{cdct}}{2r}\right)\right] r^2 - \left\{\left(r - (r - w_{cdct}/2)\right)\frac{l_{cdct}}{2}\right\}$
Eq. 29	$l_{cdcb} = 2\left[2\left(r - \frac{w_{cdcb}}{2}\right) r - \left(r - \frac{w_{cdcb}}{2}\right)^2\right] 0.5$
Eq. 30	$a_{cdct} = a_t - \frac{2}{144}\left[\left(\sin^{-1}\frac{l_{cdcb}}{2r}\right) r^2\right.$
Eq. 31	$\left. - \left\{(r - (r - w_{cdcb}/2))\frac{l_{cdcb}}{2}\right\}\right]$
Eq. 32	$l_{cdcs} = 2[2\left(r - \frac{w_{cdcs}}{2}\right) r - \left(r - \frac{w_{cdcs}}{2}\right)^2]^{0.5}$
Eq. 33	$a_{cdct} = a_t - \frac{2}{144}\left[\left(\sin^{-1}\frac{l_{cdcs}}{2r}\right) r^2\right.$
Eq. 34	$\left. - \left\{(r - (r - w_{cdcs}/2))\frac{l_{cdcs}}{2}\right\}\right]$
Eq. 35	$l_w = 2 l_w$
Eq. 36	$l_w = 2 l_w$
Eq. 37	$a_b = a_t - 2a_{dct} - \max(a_{cdcb}, a_{cdcs})$
Eq. 38	$a_{dc} = 2(a_{dct}\, a_{dcb})^{0.5}$ $a_{dct} = 2a_{dct}$
Eq. 39	$a_{dcb} = 2a_{dcb}$
Eq. 40	$l_w = 2 l_{cdct}$
Eq. 41	$a_b = a_t - 2a_{cdct} - \max(a_{dcb}, a_{dcs})$
Eq. 42	$a_{dc} = 2(a_{cdct}\, a_{cdcb})^{0.5}$
Eq. 43	$a_{sdcb} = a_{dcb}$
Eq. 44	$a_{dcb} = a_{cdcb}$
Eq. 45	$a_{sdct} = a_{dct}$
Eq. 46	$a_{dct} = a_{cdct}$

Eq. 47	$$h_w = ch_w$$
Eq. 48	$$a_b = a_t - a_{dct} - \max(a_{dcb}, a_{dcs})$$
Eq. 49	$$a_{dc} = (a_{dct}\, a_{dcb})^{0.5}$$
Eq. 50	$$u_{bdcvt}$$
Eq. 51	$$= \left[\left(\frac{u_{dfc} - \frac{q_{ldc}}{448.8a_{dct}}}{2.49}\right)\left(\frac{\rho_L - \rho_V}{\rho_V}\right)^{0.26}\left(\frac{a_{dct}}{a_{dc}}\right)^{0.4}\right]^{\left(\frac{1}{0.5}\right)}$$
Eq. 52	$$u_{bdcvw} = \left[\left(\frac{u_{dfc} - \frac{q_{ldc}}{448.8a_{dc}}}{1.379}\right)\left(\frac{\rho_L - \rho_V}{\rho_V}\right)^{0.22}\right]^{\left(\frac{1}{0.54}\right)}$$
Eq. 53	$$u_{bdcv} = \min(u_{bdcvt}, u_{bdcvw})$$
Eq. 54	$$u_b = \frac{M_V}{3600\rho_V a_b}$$
Eq. 55	$$q_{ls} = \frac{q_l u_{bdcv}}{u_b}$$
Eq. 56	$$F_r = \left[\left(\frac{12\rho_V}{(\rho_L - \rho_V)}\right)\left(\frac{u_b^2}{32.185h_{cl}}\right)\right]$$
Eq. 57	$$\eta = 13.3F_r^{0.4}\phi^{-0.25}$$
Eq. 58	$$\alpha_t = \frac{1}{1+\eta}$$
Eq. 59	$$h_f = \frac{h_{cl}}{\alpha_t}$$
Eq. 60	$$C_d = \begin{cases} 0.61 + 0.08\frac{h_f - h_w}{h_w}, & \frac{h_f - h_w}{h_w} \le 8.135 \\ 1.06(1 + \frac{h_w}{h_f - h_w})^{1.5}, & otherwise \end{cases}$$
Eq. 61	$$h_{cl} = \alpha_t h_w + 1.02\left(\frac{\alpha_t^{0.5}}{C_d}\right)^{0.67}\left(\frac{q_l - q_w}{l_w}\right)^{0.45}$$
Eq. 62	$$\Delta P = 5.28u_b^2\left(\frac{1-\phi^2}{\phi^{0.2}}\right)\left(\frac{d_h}{deck_t}\right)^{0.2}\left(\frac{\rho_V}{32.185\rho_L\phi^2}\right) + h_{cl}$$
Eq. 63	$$WFP = \begin{cases} \frac{(l_w + \max(l_{dcb}, l_{dcs}) + 12d_t}{3}, & forpass = \\ \frac{(l_w/2 + \max(l_{cdcb}, l_{cdcs})}{2}, & forpass = \\ \frac{(l_{cdct} + \max(l_{dcb}, l_{dcs})}{2} & forpass = \end{cases}$$
Eq. 64	$$a_h = \phi a_b$$
Eq. 65	$$a_h = \phi a_b$$
Eq. 66	$$u_l = \frac{q_l - q_w}{3.116h_{cl}WFP}$$
Eq. 67	$$weep_{df} = \frac{h_{cl}}{\alpha_t} - \Delta P$$

Eq. 68	$u_{BWP} = \left(\frac{14.5\phi^{1.44}}{\rho_V^{0.5}}\right)\left(\frac{\rho_L-\rho_V}{\rho_V}\right)^{0.094}\left(\frac{d_h}{deck_t}\right)^{-0.22}(\rho_L h$
Eq. 69	$q_{w1} = \max(q_{w2}, 0)$
Eq. 70	$q_{w2} = \begin{cases}(94.6a_h\alpha_t^2)\left(e^{\left(\frac{-0.043u_l d_h}{deck\ t}\right)}\right)\left(1-\left[\frac{u_b}{u_{BWP}}\right]^{0.5}\right)\left(64.37\left[\frac{h_{cl}}{\alpha_t}\right.\right. \\ 0,\end{cases}$
Eq. 71	$q_{w1} = \max(q_{w2}, 0)$
Eq. 72	$q_{w2} = \max(q_{w2}, 0.9q_l)$
Eq. 73	$q_w = \frac{q_{w1}+q_{w2}}{2}$
Eq. 74	$q_{w1} = q_{w2}$
Eq. 75	$q_{ldc} = q_{ls} - q_w$
Eq. 76	$u_{bdcvt} = \left[\left(\frac{\left[u_{dfc} - \frac{q_{ldc}}{448.8a_{dct}}\right]}{2.49}\right)\left(\frac{\rho_L-\rho_V}{\rho_V}\right)^{0.26}\left(\frac{a_{dct}}{a_{dc}}\right)^{0.4}\right]^{\bar{0}}$
Eq. 77	$u_{bdcvw} = \left[\left(\frac{\left[u_{dfc} - \frac{q_{ldc}}{448.8a_{dc}}\right]}{1.379}\right)\left(\frac{\rho_L-\rho_V}{\rho_V}\right)^{0.22}\right]^{\frac{1}{0.54}}$
Eq. 78	$u_{bdcv2} = \min(u_{bdcvt}, u_{bdcvw})$
Eq. 79	$u_{bdcv} = u_{bdcv2}$
Eq. 80	$u_{bdcv} = \frac{u_{bdcv1}+u_{bdcv2}}{2}\ u_{bdcv1} = u_{bdcv2}$
Eq. 81	$a_f = \begin{cases}a_t - 0.5(a_{dct}+a_{dcb}), & forpass = 1 \\ a_t - 0.5(a_{cdct}+a_{cdcb}), & forpass = 2A \\ a_t - 0.5(a_{sdct}+a_{sdcb}) & forpass = 2B\end{cases}$
Eq. 82	$c_b = u_b\left[\frac{\rho_V}{\rho_L-\rho_V}\right]^{0.5}$
Eq. 83	$c_{bfl} = 0.9\left[\frac{\rho_V}{\rho_L-\rho_V}\right]^{0.04}\left[e^{\frac{-11}{S_{tray}}}\right]\left[\frac{a_f}{a_b}\right]^{0.5}\left[e^{\frac{0.68}{d_h+0.73+0.24\left(\frac{q_L}{l_w}\right.}}\right. - \frac{1}{e^{\phi^{0.23}\left(\frac{q_l}{l_w}+0.25\right)^{0.2}}}\left.\right]\left[e^{-0.6\left(\frac{S_{tray}\ l_w}{6q_L}\right)^2}\right]$
Eq. 84	$c_s = \left[\frac{M_V}{3600\rho_V a_t}\right]\left[\frac{\rho_V}{\rho_L-\rho_V}\right]^{0.5}$
Eq. 85	$u_{lv} = \left[\frac{M_L}{3600\rho_L a_t}\right]$
Eq. 86	$c_{sp} = \frac{1.4\left[\frac{\sigma}{\rho_L-\rho_V}\right]^{0.2}\left[\frac{\rho_V}{\rho_L-\rho_V}\right]^{-0.5}}{1+1.4\left[\frac{\rho_V}{\rho_L-\rho_V}\right]^{-0.5}}$
Eq. 87	$c_{ss} = 0.641c_{sp}e^{\left[-11.25\left(\frac{u_{lv}-0.033}{c_{sp}}\right)^2\right]}$

Eq. 88	$$p_{vsl} = 100\frac{c_s}{c_{ss}}$$
Eq. 89	$$c_{afo} = \begin{cases} 0.0263S_{tray} - \left(\left(0.58 - \frac{3.29}{S_{tray}}\right) - \left(\frac{S_{tray}\,\rho_V - S_{tray}}{1560}\right)\right), \\ \left(0.58 - \frac{3.29}{S_{tray}}\right) - \left(\frac{S_{tray}\,\rho_V}{23.88S_{tray} + 987}\right) + \left(\end{cases}$$
Eq. 90	$$\text{If} \quad c_{afo} > \frac{S_{tray}{}^{0.65}}{12}\rho_V{}^{0.167} \quad \text{then,} \quad c_{afo} = \frac{S_{tray}{}^{0.65}}{12}\rho_V{}^{0.167}$$
Eq. 91	$$\text{If} \quad c_{afo} > 0.28[1.1 - 0.14\rho_V] + 0.3 \quad \text{then,} \quad c_{afo} = 0.28[1.1 - 0.14\rho_V] + 0.3$$
Eq. 92	$$v_{load} = c_b a_b$$
Eq. 93	$$AUD = \begin{cases} l_{dcb}\,c_{dc}, & forpass = 1 \\ 2l_{dcb}\,c_{dc}, & forpass = 2A \\ 2l_{cdcb}\,c_{cdc} & forpass = 2B \end{cases}$$
Eq. 94	$$FPL = \begin{cases} 12d_t - w_{dct} - \max(w_{dcb}, w_{dcs}), & fo \\ 6d_t - w_{dct} - 0.5\max(w_{cdcb}, w_{cdcs}), & fo \\ 6d_t - 0.5w_{dct} - \max(w_{dcb}, w_{dcs}) & fo \end{cases}$$
Eq. 95	$$HLUDC = \begin{cases} 0.06\left[\frac{q_l}{l_{dcb}\,c_{dc}}\right]^2, & forpass = 1 \\ 0.06\left[\frac{q_l}{2l_{dcb}\,c_{dc}}\right]^2, & forpass = 2A \\ 0.06\left[\frac{q_l}{2l_{cdcb}\,c_{cdc}}\right]^2 & forpass = 2B \end{cases}$$
Eq. 96	$$gmpjf = 100\frac{vload + \frac{q_l FPL}{13000}}{a_b\,cafo}$$
Eq. 97	$$FID = \frac{q_l}{a_{dct}}$$
Eq. 98	$$\%Downcomerflood = 100\max\left(\frac{FID}{250}, \frac{FID}{41(\rho_L - \rho_V)^{0.5}}, \frac{FID}{5(\rho_L - \rho_V)^{0.5}S_{tray}^{0.5}}\right)$$
Eq. 99	$$weirload = \frac{q_l}{l_w}$$
Eq. 100	$$DCBU = \hbar_w + 0.4\,weirload^{0.66} + (dp + HLUDC)\left(\frac{\rho_L}{\rho_L - \rho_V}\right)$$
Eq. 101	$$\%Downcomerbackup = 100\frac{DCBU}{S_{tray}}$$
Eq. 102	$$fmpjfl = 100\frac{c_b}{c_{bfl}}$$
Eq. 103	$$\%Jetflood = \begin{cases} fmpjflforvtype = 0 \\ gmpjfforvtype = ot\hbar ers \end{cases}$$
Eq. 104	$$u_{ldc} = \frac{M_L}{3600a_{dct}\,\rho_L}$$
Eq. 105	$$dpdry = dp - \hbar cl$$
Eq. 106	$$dppsi = \frac{dp\rho_L}{1728}$$

Eq. 107	$$wfrac = \frac{q_w}{q_l}$$
Eq. 108	$$c_{bfspec} = c_{bfl}$$
Eq. 109	$$c_{bfspec} = \frac{100c_b}{gmpjf} if vtype > 0$$
Eq. 110	$$c_{bespec} = \max(c_b, 0.5c_{bfspec})$$
Eq. 111	$$efrac = \min\left(0.10\left[\frac{c_{bespec} - c_{bfspec}}{\left[\frac{\rho}{\rho L - \rho V}\right]^{-0.2}} \frac{1}{31 + 31\frac{pl}{lw}}\right], 1\right)$$
Eq. 112	$$efrac = efrac\frac{M_V}{M_L} if M_V > M_L$$

REFERENCES

[1] Kister HZ. Distillation design, McGraw Hill, CA 1992.

[2] Sinnot RK. Coulson and Richardson's Chemical engineering-Chemical engineering design, Butterworth-Heinemann, Oxford, UK; Second edition 1989; 6.

[3] Luyben WL. Distillation design and control using aspen simulation, John Wiley and sons inc, NJ 2006. http://dx.doi.org/10.1002/0471785253

[4] Kennedy J and Eberhart RC. Particle swarm optimization, in: Proc. of IEEE International Conference on Neural Networks, Piscataway, NJ 1995; 1942-1948. http://dx.doi.org/10.1109/ICNN.1995.488968

[5] Dorigo M. Optimization, Learning and Natural Algorithms (in Italian). PhD thesis; Dipartimento di Elettronica, Politecnico di Milano, IT 1992.

[6] Dorigo M, Caro DG and Gambardella LM. Ant Algorithms for Discrete Optimization, Artificial Life 1999; 3(5): 137-72. http://dx.doi.org/10.1162/106454699568728

[7] Shelokar PS, Siarry P, Jayaraman VK and Kulkarni BD. Particle swarm and ant colony algorithms hybridized for improved continuous optimization, Applied Mathematic Computation 2007; 188: 129-142. http://dx.doi.org/10.1016/j.amc.2006.09.098

[8] Angeline P. Evolutionary optimization versus particle swarm optimization: philosophy and performance difference. Proceeding of the Evolutionary Programming Conference; San Diego, USA 1998. http://dx.doi.org/10.1007/bfb0040811

[9] Kaveh A and Talatahari S. A hybrid particle swarm and ant colony optimization for design of truss structures, Asian journal of civil engineering (building and housing) 2008; 9(4): 329.

[10] Mozafari B, Ranjbar TAM, Amraee M, Mirjafari AR and Shiranib. A hybrid of particle swarm and ant colony optimization algorithms for reactive power market simulation, Journal of Intelligent and Fuzzy Systems 2006; 6(17): 557-74.

[11] Pinto FS, Zemp R, Jobson M and Smith R. Thermodynamic optimization of distillation columns, Chemical Engineering Science 2011; 66: 2920-2934 http://dx.doi.org/10.1016/j.ces.2011.03.022

[12] Lahiri SK. Particle Swarm Optimization Technique for the Optimal Design of Plate-Type Distillation Column. Applications of Metaheuristics in Process Engineering, Springer, Switzerland 2014.

[13] Ponce-Ortega JM, Serna M. and Jimenez A. Applied Thermal Engineering 2009; 29: 203-209. http://dx.doi.org/10.1016/j.applthermaleng.2007.06.040

Received on 24-02-2016 Accepted on 16-03-2016 Published on 31-07-2016

DOI: http://dx.doi.org/10.15377/2409-983X.2016.03.01.1